AN AIRBORNE INTERFEROMETRIC SAR SIMULATOR

G. Alberti[1], S. Esposito[1], A. Moccia[2] and S. Vetrella[1]

[1] CO.RI.S.T.A. Consortium
[2] Faculty of Engineering, University of Naples "Federico II"

ABSTRACT

This paper presents an airborne SAR interferometer simulator which uses a coherent approach based on a pulse-by-pulse synthesis in time domain and takes into account the sensor parameters and its observation geometry as well as the trajectory and attitude dynamics of the aircraft. Preliminary experimental results are presented in order to assess the interferometric simulator performance in terms of its transfer function and in order to analyse the effect of various contributions to the interferometric phase errors.

Keywords: SAR simulation, SAR interferometry, phase statistics.

1. INTRODUCTION

The possibility of reconstructing terrain height by means of SAR interferometry has been successfully demonstrated in recent years (Refs. 1, 2). Several elevation maps have been derived either from the processing of data provided by satellite multiple-pass pairs or by means of two antennas mounted on the same airborne platform (Refs. 3, 4, 5). Thanks to the use of a single-pass approach in order to overcome surface temporal decorrelation, the latter system has shown a better capability of producing Digital Elevation Models (DEM) over large areas with high accuracy and resolution. In order to validate the interferometric techniques, DEMs obtained by SAR interferometry must be compared to existing topographic data. Unfortunately, several operational aspects make difficult the comparison: on one hand, it is rare to have precise ground truth description of the area of interest, on the other hand the geographic projection of the interferometric DEM introduces registration errors.
An interesting validation method is offered by simulation techniques, which allow a very precise comparison between input topography and interferometric data.
In addition, an adequate simulation model makes possible the analysis of the effect of platform dynamics on the interferometric phase, in order to evaluate the overall system performance.
Finally, the possibility of varying the main system parameters, can help in the design of future mission configurations.
This paper describes an airborne interferometric SAR simulator developed by CO.RI.S.T.A. consortium and shows the preliminary results obtained by using the JPL/NASA TOPSAR parameters.

2. SIMULATION MODEL

The interferometric SAR simulator basically consists of three main blocks: scene generation, aircraft dynamic simulation and radar signal synthesis (Fig.1).

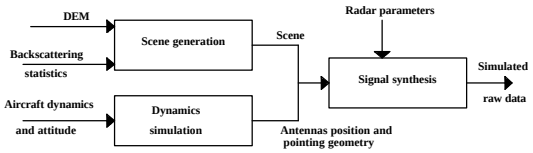

Figure 1: *Block diagram of the SAR interferometer simulator*

The output of the first block is the scene to be observed which is divided in elementary cells of arbitrary size. Each of them is characterised by its geographic co-ordinates and height, as well as by a complex voltage reflection coefficient with assigned distribution.
The trajectory and attitude of the antennas are evaluated in the second block by considering the lever arms and the orientation angles between the body reference frame (centred in the aircraft centre of mass) and the antenna reference frame (centred in the antenna phase centre). The position, velocity and yaw, pitch and roll angles of the aircraft are assigned as user-defined functions of time. The computed antenna attitude angles make possible to determine the azimuth and elevation angles of instantaneous line-of-sight of each DEM element with respect to the antenna normal, in order to account for the actual influence of the transmitting and receiving antenna patterns on the received signal.
In the last block the SAR raw signal is synthesised by using a time domain approach. In each azimuth position (spaced of prf^{-1} seconds), the echoes from each DEM element are coherently added, considering their proper phase factor and time delay. The

amplitude weights due to antenna patterns and propagation (inversely proportional to the squared distance) as well as the sampling effects are taken into account. After heterodyning and considering a null video-offset frequency, the simulated SAR signal received in the j-th azimuth position is given by:

$$s_j(t) = \sum_{i \in DEM} \sigma_i w_{i,j} \exp\left[-j \frac{4\pi}{\lambda} r_{i,j} + \alpha (t - t_0)^2 \right] \Pi\left(\frac{t - t_0}{T} \right)$$

where:
$$t_0 = \frac{2 r_{i,j}}{c} - rgd - \frac{T}{2}$$

$$\Pi\left(\frac{t}{T} \right) = \begin{cases} 1 & |t| < \frac{T}{2} \\ 0 & \text{elsewhere} \end{cases}$$

rgd being the range gate delay, T being the pulse duration, α being the chirp rate, σ_i being the complex backscattering coefficient of the i-th DEM element, $w_{i,j}$ being the pattern antenna weight and $r_{i,j}$ being the distance between the j-th azimuth position of the antenna and the i-th DEM element, c being the velocity of the light and λ being the wavelength.
The output of the simulator is a pair of interferometric SAR raw-data which must be adequately processed in order to derive the final height information. A single antenna compressed image and the resulting interferogram are shown in Fig. 2.
This simulation concerns the JPL TOPSAR system, on board the NASA DC8, which flew over several Italian test-sites in 1991. The main system parameters used in the simulation procedure are summarised in Table 1.

aircraft speed	214.4 m/s
aircraft altitude	8000 m
prf	283.42 Hz
3 dB antenna elevation beamwidth	30 deg
3 dB antenna azimuth beamwidth	2 deg
antenna elevation angle	45 deg
chirp bandwidth	40 MHz
sampling frequency	45 MHz
wavelength	5.65 cm
pulse duration	5 μs
range gate delay	62.8 μs
Baseline components (Ref. 6)	
Bx (longitudinal)	0 m
By (lateral)	-1.180514 m
Bz (vertical)	2.294076 m

Table 1 : *Main simulation parameters*

The simulated DEM consists of 1000x1000 elements which cover an area of 500x1500 meters in range and azimuth directions, respectively. Each cell has been modelled as an isotropic and stationary scatterer, characterised by a complex coefficient with Rayleigh-distributed amplitude and uniform distributed phase in the interval [0, 2π[. By changing the mean of the amplitude distribution according to the ratio of 5:3, two homogeneous areas have been generated (Fig. 2).
The noise introduced by the SAR amplification chain has been modelled as additive, gaussian, and white (AWGN). Therefore it has been added to the simulated raw-data in order to obtain a signal to noise ratio (SNR) of 17.42 dB and 13 dB respectively in the upper and lower area of the compressed images. For this purpose, the processor equivalent noise bandwidth has been evaluated by considering a calibrated gaussian white noise as input.
Finally, to validate the procedure by means of a comparison with analytical models, a straight flight path with constant speed and altitude and a flat test-area have been simulated.

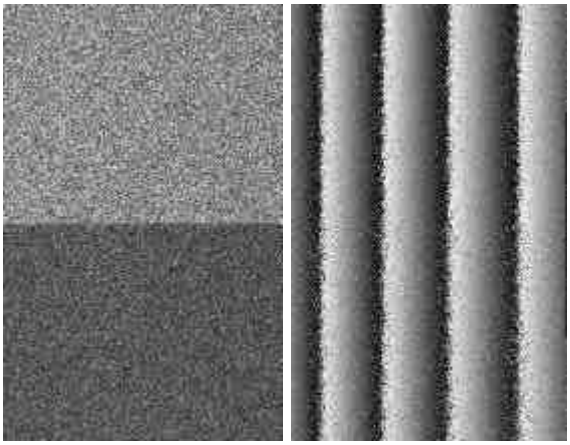

Figure 2 : *Simulated image and interferogram*

3. SIMULATION RESULTS

In this paragraph the results obtained by analysing the statistics of the simulated signals are presented.
The key issue of an interferometric SAR simulator is the synthesis of an accurate speckle statistics. Indeed, by increasing the accuracy in the knowledge of system parameters, the interferometric errors are mainly due to the resulting speckle statistics. The adopted simulation approach is based on a pulse-by-pulse synthesis in time domain and, consequently, produces the speckle statistics in a straightforward way, by coherently adding the echo from each DEM element computed with its proper phase factors.
Fig. 3 shows the two dimensional autocorrelation function of simulated raw-data in which, as expected, a spatial correlation due to the shape of simulator transfer function (STF) is evident. In range direction the autocorrelation function is very similar to the STF since the weight introduced by the antenna pattern is

quite constant over the observed scene, while in azimuth direction a larger broadening effect can be noted due to a greater pattern modulation. The measurements done on the autocorrelation function show a 3 dB beamwidth equal to 1.21 resolution elements in azimuth direction and to 1.06 resolution elements in range direction.

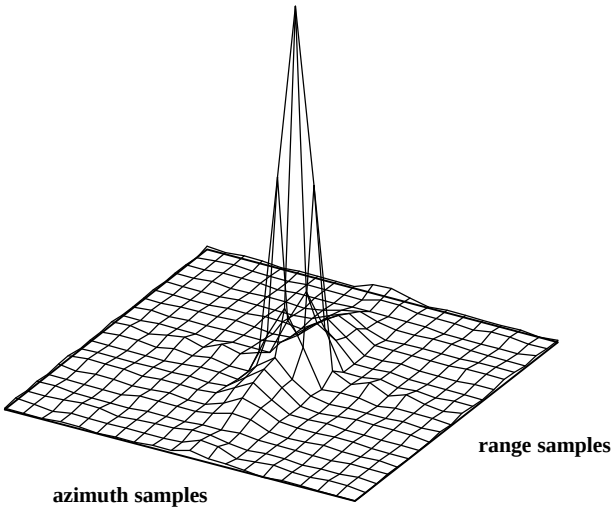

Figure 3 : *Autocorrelation function of simulated raw-data*

As far as the interferogram statistics is concerned, the measured probability density function (pdf) of simulated phase differences ($\Delta\varphi$) is plotted in Fig. 4. For this purpose, the phase pattern due to constant height has been removed by applying an appropriate compensation to the interferogram.
This pdf is known in the more general contest of second order speckle statistics (Ref. 7) and its theoretical expression is given by:

$$\mathrm{pdf}(\Phi) = \frac{1-|\gamma|^2}{2\pi}\frac{1}{1-|\gamma|^2\cos^2\Phi}\left\{1+\frac{|\gamma|\cos\Phi\arccos(-|\gamma|\cos\Phi)}{\sqrt{1-|\gamma|^2\cos^2\Phi}}\right\} \quad (1)$$

where: $\Phi = \Delta\varphi - \arg(\gamma)$

$\Delta\varphi$ being the phase difference.
In the previous formulation the parameter γ expresses the degree of coherence between the complex values of the two images z_1 and z_2, and it is defined as:

$$\gamma = \frac{E(z_1 z_2^*)}{\sqrt{E(z_1^2)E(z_2^2)}}$$

Assuming flat terrain and separable point spread function, the correlation coefficient γ can be evaluated as (Ref.8):

$$\gamma_{th} = \frac{\alpha}{1+\mathrm{SNR}^{-1}} \quad (2)$$

where:

$$|\alpha| = (1-|a_x|)(1-|a_r|)\,\mathrm{sinc}\left[\frac{\delta_x}{X}(1-|a_x|)\right]\mathrm{sinc}\left[\frac{\delta_r}{R}(1-|a_r|)\right]$$

$$\arg\{\alpha\} = \pi\frac{\delta_x}{X}|a_x| + \pi\frac{\delta_r}{R}|a_r|$$

$$a_x = \frac{B_x X}{r\lambda}$$

$$a_r = \frac{B_y R}{r\lambda\sin\theta}$$

R and X being the theoretical resolutions in range and azimuth direction respectively, δ_r and δ_x being the registration errors between the two images in range and azimuth direction respectively, r being the slant range, θ being the elevation angle. The $|\gamma|$ obtained from Eq.2, after integration to account for varying r, has been chosen as a reference value, since our simulation configuration matches very well the hypothesis on which Eq.2 is based.

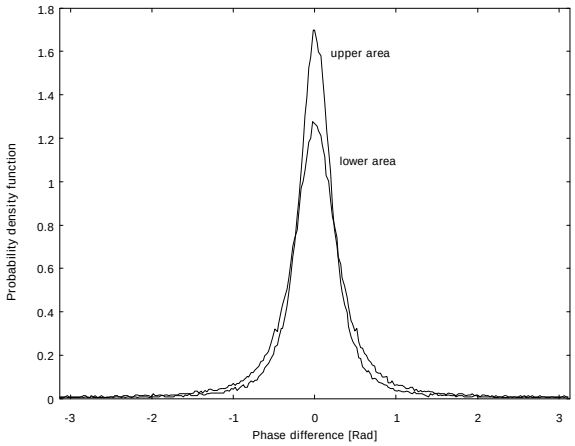

Figure 4 : *Pdf of the phase differences*

In order to validate the pdf of simulated phase difference, the value of $|\gamma|$ computed by inverting Eq.1 has been compared to the reference one. The results are shown in table 2.

	reference $\|\gamma\|$	computed $\|\gamma\|$
Upper area	0.953	0.958
Lower area	0.924	0.928

Table 2 : *Comparison between correlation coefficients*

Obviously, the different values of $|\boldsymbol{\gamma}|$ between the two simulated homogeneous areas, due to the adopted SNRs and in accordance with Eq.2, explain the presence of two pdf plots in Fig. 4.
As mentioned earlier, the uncertainty of the phase difference ($\boldsymbol{\sigma_{\Delta\varphi}}$) determines the uncertainty of the height computed by means of SAR interferometry ($\boldsymbol{\sigma_h}$). In fact, in the case of exact knowledge of baseline components, aircraft altitude, straight flight trajectory with constant velocity, $\boldsymbol{\sigma_h}$ is given by:

$$\sigma_h = \frac{r^2 \lambda \sin\theta}{2\pi q(r+p)} \sigma_{\Delta\varphi} \qquad (3)$$

where:

$$p = B_z \cos\theta - B_y \sin\theta$$
$$q = B_z \sin\theta + B_y \cos\theta$$

Table 3 shows the $\boldsymbol{\sigma_h}$ values measured on the output DEM and the reference values evaluated from Eq.3 with $\boldsymbol{\sigma^2_{\Delta\varphi}}$ given by the numerical integration of $\Phi^2 \mathrm{pdf}(\Phi)$.

	reference $\boldsymbol{\sigma_h}$	computed $\boldsymbol{\sigma_h}$
Upper area	14.1 m	13.3 m
Lower area	17.2 m	16.8 m

Table 3 : *Height uncertainty comparison*

Fig.5 shows the pdf of the output height image which, as expected, is a scaled version of the phase difference one (Fig.4).

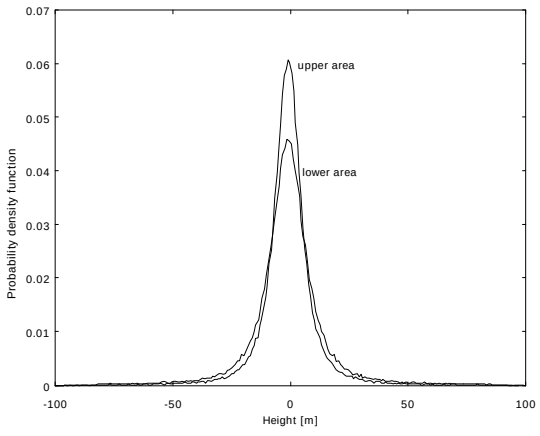

Figure 5 : *Pdf of the computed heights*

As final validation, the statistics of the simulated data have been analysed after a multi-look processing. The adopted technique is a coherent multi-look in time domain which has been proved to be a maximum-likelihood estimator (MLE) of interferometric phase for homogeneous targets (Ref.9). In this case, the Cramer-Rao bound for the interferometric phase standard deviation is (Ref.9):

$$\sigma_{\Delta\hat{\varphi}} = \frac{\sqrt{1-\gamma^2}}{\gamma\sqrt{2N_L}}$$

where N_L is the number of looks and $\Delta\hat{\varphi}$ is the estimated phase difference. The actual phase standard deviation approaches this limit asymptotically as the number of looks increases. Fig.6 presents a comparison of the phase standard deviation measured on the simulated interferogram against the Cramer-Rao bound for various values of the number of looks.

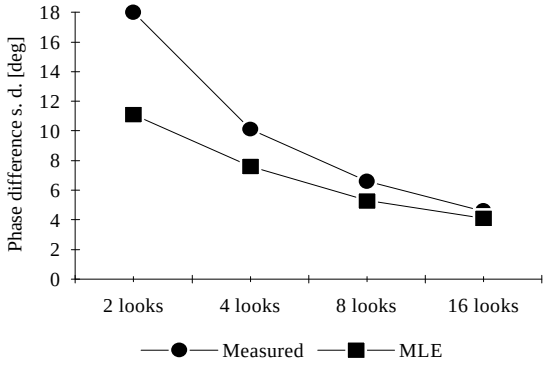

Figure 6 : *Phase standard deviation comparison*

The percent error of Cramer-Rao estimator decreases from 38% to 12% by increasing the number of looks from 2 to 16, in accordance with the results available in literature (Refs. 8, 9). It is worth noting that the height uncertainty measured on the 16-looks interferogram reaches 1.7 m and 2.2 m on the upper and lower area respectively.

4. CONCLUSION

This paper presented an airborne SAR interferometer simulator developed at consortium CO.RI.S.T.A. The adopted model uses a coherent approach based on a pulse-by-pulse synthesis in time domain and takes into account the sensor parameters and its observation geometry as well as the trajectory and attitude dynamics of the aircraft.
By using the TOPSAR parameters and homogeneous flat terrain, a pair of interferometric raw-data have

been simulated and the relative interferogram has been produced by processing the data. The phase statistics of the simulated data have been analysed and the experimental results showed a satisfactory agreement with those available in literature.
Our future research activity will deal with the simulation of aircraft dynamics, in order to develop and validate suitable procedure for motion compensation and interferometric phase calibration.

ACKNOWLEDGEMENTS

This paper has been carried out under the sponsorship of Italian Space Agency (ASI).

5. REFERENCES

1. Gabriel, A. K, and Goldstein, R. M., 1988, Crossed orbit interferometry: theory and experimental results from SIR-B. *International Journal of Remote Sensing*, Vol. 9, No. 8, pp.857-872.

2. Graham, L. C., 1974, Synthetic Interferometer Radar For Topographic Mapping. *Proceedings of the IEEE*, Vol. 62, No. 6, pp. 763-768.

3. Zebker, H. A., Madsen, S. N., Martin, J., Wheeler, K. B., Miller, T., and Lou, Y., Alberti, G., Vetrella, S. and Cucci, A., 1992, The TOPSAR Interferometric Radar Topographic Mapping Instrument. *IEEE Transactions on Geoscience and Remote Sensing*, Vol. 30, No. 5, pp. 933-940.

4. Prati, C., Rocca, F., Monti Guarnieri, A., and Damonti, E., 1990, Seismic Migration for SAR Focusing: Interferometrical Applications. *IEEE Transactions on Geoscience and Remote Sensing*, Vol. 28, No. 4, pp. 627-640.

5. Zebker, H. A., and Goldstein, R. M., 1986, Topographic Mapping From Interferometric Synthetic Aperture Radar Observations. *Journal of Geophysical Research*, Vol. 91, No. B5, pp. 4993-4999.

6. Alberti G., Vetrella S., Moccia A., Ponte S. 1993, Analysis and results of the TOPSAR experiment in southern Italy, accepted for publication in *EARSeL Advances in Remote Sensing*

7. Goodman j. w., Statistical properties of laser speckle patterns, in *Laser speckle related phenomena*. Ed. J. C. Dainty, Springer, 1975

8. Rodriguez, E., Martin, J. M., 1992, Theory and design of interferometric synthetic aperture radars. *IEE Proceedings*, Vol. 139, No. 2, pp. 147-159.

9. Rodriguez, E., Maximum likelihood estimation of interferometric phase from distributed targets, *IEEE Transaction on Geoscience and Remote Sensing* (to be published)